Article

Spectroscopic studies of oxide interfaces in aquatic geochemical systems

Peter J. Swedlund

School of Chemical Sciences, University of Auckland, Private Bag 92019, New Zealand
(email: *p.swedlund@auckland.ac.nz)*

Keywords: *aquatic geochemistry, iron oxides, interfacial silicate polymerisation*

Setting the scene

Geochemistry has been described as the study of the chemical forces that determine the distribution of elements in the Earth.[1] Even though 95 % of the volume of the Earth's crust is comprised of close-packed oxygen ions, there is a rich diversity of minerals based on the variety of cations and the numerous ways these cations can be arranged within the oxygen ion lattice. Silicon is the main cation with a crustal abundance of 28 % (by mass) followed by Al, Fe, Ca, Mg, Na, and K with crustal abundance in mass % of 8.4, 5.1, 4.6, 2.7, 2.4 and 1.6 respectively.[2] Carbon, which is so prominent in so much chemistry, doesn't even make the 1st XV in crustal abundance.

Silicate phases make up 90 % of the Earth's crust and, with few exceptions, contain SiO_4 tetrahedra. These tetrahedra exist with varying degrees of polymerisation via Si-O-Si linkages where a given Si is designated as Q^n where n is the number of Si–O–Si linkages present. Silicate minerals range from having isolated SiO_4^{4-} anions, the Q^0 orthosilicates, to those with polymerisation in three dimensions, the Q^4 tectosilicates. The silicon-oxygen bond has unusual characteristics and warrants some introduction. Unlike the ubiquitous ketones in carbon chemistry, the first silanone compound (i.e. with a Si=O) was only recently reported.[3] The instability of Si=O explains the marked difference in the properties of CO_2 and SiO_2. The Si-O single bond has been subject to much historical debate[4] and even for the simple molecule of disiloxane ($H_3Si\text{-}O\text{-}SiH_3$) a full explanation for the anomalous basicity compared to its carbon analogue, dimethyl ether, was only recently reported and illustrates some interesting chemistry.[5] For $H_3X\text{-}O\text{-}XH_3$, the lower electronegativity of Si than C explains the larger X-O-X bond angle when X = Si, as expected from Bent's rule whereby less electronegative substituents bind to hybrid orbitals with less p character. However, the lower basicity of the oxygen in $H_3S\text{-}O\text{-}SiH_3$ than $H_3C\text{-}O\text{-}CH_3$ is unexpected from the difference in electronegativity but arises because the larger X-O-X bond angle for X = Si enhances vicinal hyperconjugation which removes electron density from the oxygen.[5]

Geochemistry covers extremely diverse conditions and processes that occur on phenomenal scales in time and space. In the fiery bowels of the Earth, the formation of assemblages of minerals (i.e. rocks) occurs as magma cools and the distribution of the elements depend on subtle chemistry relating to the stability and miscibility of phases at high temperatures and pressures. The mountain tops are the other extreme of both temperature and the life cycle of rock. Tectonic forces thrust rocks up into the weather where they meet their fate under the influences of O_2 and water which, by a combination of physical, chemical and biological weathering, eventually converts rock to soils. Subduction returns weathered surface material to the furnace and completes the rock cycle process.

Weathering, iron oxides and H_4SiO_4

The distribution of elements during weathering of minerals is determined by the aqueous solubility of the cations. Of the dominant cations in the crust, the Group I and II cations are extremely soluble, while exposure to 0.2 atm of O_2 results in the Fe^{2+} cation in silicate minerals being oxidised to Fe^{3+}. In water at pH 7 and at 25 °C, the solubility of Si^{4+} (as H_4SiO_4 or silicic acid) with respect to an amorphous SiO_2 phase is 1.8 mM while the solubilities of Al^{3+} and Fe^{3+} with respect to amorphous oxyhydroxide phases are respectively 7.9 mM and 0.28 nM.[6] Therefore, the weathering process ultimately coverts silicate minerals to the oxyhydroxides of Al^{3+} and Fe^{3+} with the aluminosilicate clays being intermediate phases. Given the economic importance of iron and aluminium oxides, the difference in the New Zealand and Australian economies is in some ways a difference in the extent of weathering reactions.

The iron oxide phases give the weathered solids of the Earth (i.e. the soils and sediments, their characteristic brown, yellow and red colours). In addition, the iron oxides often play an important role in the aqueous geochemistry of many cationic, anionic, and neutral species, including many environmentally important trace elements. This was elegantly demonstrated by John Aggett at the University of Auckland who determined the phase association of arsenic accumulated on lake sediments using an EDTA solution to cause the slow dissolution of the metal oxide phases in the sediment over 48 h.[7] A comparison of the dissolution rates of As and the major solid phase cations (Fe, Al, Mn and Ca) demonstrated a clear phase association of the solid phase As with the iron oxides in the sediment. This was one of the early definitive indicators of the importance of iron oxides in determining arsenic mobility in aquatic systems which has far reaching implications for global population health.[8] In general, it is found that anions which are the conjugate bases of strong acids (such as nitrate and chloride) have a low affinity for metal oxides, while weak acids and their conjugate bases, such as H_4SiO_4, $HAsO_4^{2-}$ and HPO_4^{2-}, have a high affinity for metal oxide surfaces.

Silicic acid derives from the weathering reactions which produce the iron oxides and typical concentrations of H_4SiO_4 in aqueous systems (≈ 0.1 to 1 mM) are higher

than those of many other adsorbing ligands. For this reason iron oxides in weathered systems can contain large amounts of silicon.[9] The presence of adsorbed H_4SiO_4 affects many aspects of the geochemistry of iron oxides including the Point of Zero Charge,[10] phase stability, morphology,[11-13] and colloid stability.[14] Understanding the chemistry of H_4SiO_4 on iron oxide surfaces is therefore important in numerous systems including catalytic supports,[15] corrosion science,[16] and wastewater treatment,[17] in addition to many natural aquatic systems.[18]

Before discussing the *in situ* infrared spectroscopy of H_4SiO_4 chemistry at the aqueous-iron oxide interface it is necessary to consider the H_4SiO_4 species in aqueous solution. A strong feature of H_4SiO_4 chemistry in aquatic systems is a high propensity for polymerisation via Si-O-Si linkages. In concentrated silicate solutions at high pH a total of 48 different silicate anions are identified and range from isolated monomers to a complex array of cyclic and cage structures.[19] Early spectroscopic and potentiometric studies indicated that oligomeric silicates were significant species in the aqueous chemistry of H_4SiO_4 at neutral pH [20,21] but more recent work has shown that monomeric H_4SiO_4 is more than 99 % of the total amount of Si in solution at neutral pH.[22] Another important aspect of H_4SiO_4 aquatic chemistry is the limit on solubility. Quartz is the least soluble SiO_2 phase with a solubility product (K_{SP}) of 10^{-4} meaning that a system with 0.1 mM H_4SiO_4 is saturated with respect to quartz. However, quartz does not precipitate at ambient temperatures for kinetic reasons in aquatic systems and H_4SiO_4 solubility is limited to 1.8 mM by precipitation of an amorphous SiO_2 phase.

Infrared spectroscopy is particularly useful for the study of H_4SiO_4 chemistry on the surfaces of iron oxides because the shape of the Si–O stretching modes, n(Si–O), for the sorbed H_4SiO_4 provides insight on the symmetry of the surface complex[23] while the position of the Si–O stretching modes provides insight on the degree of silicate polymerisation.[24,25] However, water is a very strong absorber of IR radiation and the applicability of IR to the study of the metal oxide–water interface has been dramatically improved by the advent of Attenuated Total Reflectance IR (ATRIR) which provides a sampling method with the required short path length.

Some ATRIR spectra

The most prominent feature in the ATRIR spectrum of H_4SiO_4 in solution is a symmetrical band at 939 cm^{-1} due to the asymmetric Si-O stretching mode. There is also a weak and broad Si-O-H bending mode at 1100 cm^{-1} while the O-Si-O bending modes occur below the wavelength limit of the ATR crystal and the O-H stretching modes are not apparent due to the strong absorbance by H_2O. In the Raman spectrum of H_4SiO_4 in solution there is one band at 787 cm^{-1} due to the symmetric Si-O stretching mode. An interesting feature of these spectra is the shift in band position upon deuteration. For D_4SiO_4 in D_2O the symmetrical Si-O stretch shifts to lower frequency as expected from Hooke's law and the increase in mass given that the H(D) is displaced with the oxygen in the stretching modes. However, the frequency of the asymmetrical stretch in the ATRIR spectrum makes a counter-intuitive shift to higher frequency.[26] A computational study to decipher the reasons for this counterintuitive shift revealed that deuteration caused the Si-O-D bending modes to shift to lower frequency allowing them to couple with the Si-O stretching mode. This coupling is responsible for the unexpected blue shift of the stretching modes.[26]

To measure the *in situ* infrared spectra of H_4SiO_4 chemistry at the aqueous-iron oxide interface, a few microliters of an iron oxide suspension is deposited on the ATRIR crystal. The water is allowed to dry and the oxide phase adheres to the surface of the crystal and a flow cell is clamped over the crystal. Initially water at pH 11 is pumped through the flow cell which causes any carbonate on the oxides surface to desorb as evidenced by negative peaks at 1350 and 1467 cm^{-1} that grow over time until all carbonate has been removed. After this time a NaCl electrolyte solution at the desired pH and ionic strength is pumped through the cell to equilibrate the oxide under the desired set of conditions. A background ATRIR spectrum is recorded and then the desired concentration of H_4SiO_4 is added to the electrolyte which is pumped over the oxide and ATRIR spectra are recorded over time as the oxide reacts with the H_4SiO_4.

Typical spectra demonstrating the main features of the system are shown in Fig. 1 for a system where the poorly ordered iron oxide ferrihydrite reacts with 0.91 mM H_4SiO_4 at pH 4. The absorbance in the n(Si-O) region of the spectra increases over time as the surface coverage

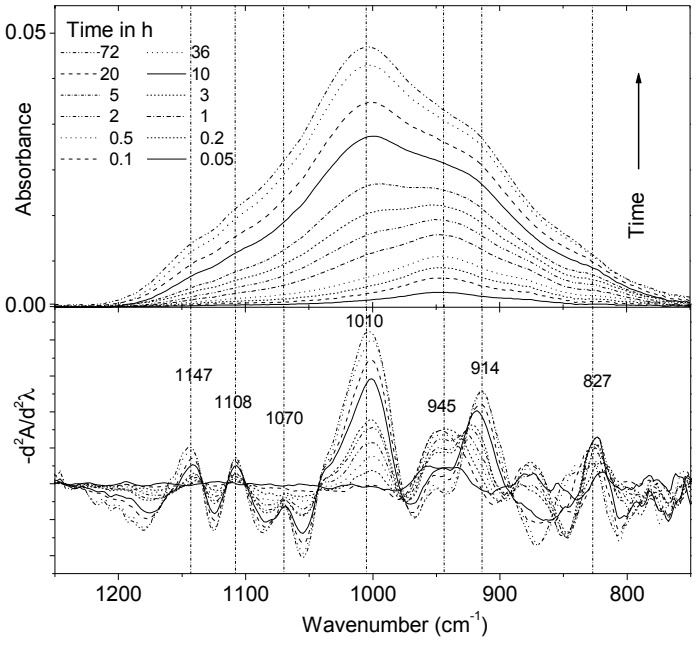

Fig 1. Top: The ATRIR spectra measured over time as 0.91 mM H_4SiO_4 in 0.01M NaCl at pH 4 reacts with a ferrihydrite film. Bottom: The negative second derivatives (Savitsky-Golay 2nd derivatives, 15 point, order 3) of the spectra in the upper panel.

(termed G_{Si}) increases but even after 3 minutes of reaction time the absorbance in the n(Si-O) region of the spectrum is > 20 times larger than the IR absorbance of the H_4SiO_4 in solution. This occurs because the ferrihydrite film on the ATRIR crystal surface is located in the few micrometres of the IR attenuating beam and demonstrates the concentration of H_4SiO_4 associated with the ferrihydrite surface compared to the same volume of water. The spectra collected immediately after the introduction of H_4SiO_4, at low G_{Si}, had a maximum at ~945 cm^{-1} with a shoulder at ~880 cm^{-1} (clearly seen in the second derivatives of these spectra). The position and shape of the spectra with H_4SiO_4 on ferrihydrite at low G_{Si} is indicative of a monomeric adsorbed silicic acid species. Compared to the IR spectra of H_4SiO_4 in solution with one n(Si-O) band at 939 cm^{-1}, the H_4SiO_4 symmetry is lowered by adsorption and spectra are consistent with a bidentate mode of attachment where the SiO_4 tetrahedra share corners with two edge-sharing Fe octahedra (Fig. 2). This is also consistent with Fe K-edge extended X-ray absorption fine structure studies of Fe(III) hydrolysed in the presence of H_4SiO_4.[27]

As the G_{Si} on ferrihydrite increases an ATRIR band at 1010 cm^{-1} grows and becomes the dominant feature in the spectra. In the second derivatives of these spectra there are bands located at 827, 914, 1070, 1108 and 1147 cm^{-1} that are associated with the main feature at 1010 cm^{-1}. The shift in the (Si-O) to higher wavenumber as G_{Si} increases is indicative of H_4SiO_4 polymerisation. However, the regular position of the band maxima in the second derivative spectra over time is quite striking and indicates that there is a single silicate species that develops as surface coverage increases and dominates the surface chemistry at high surface coverage. Comparing the shape of the IR spectra of H_4SiO_4 on ferrihydrite at high G_{Si} to the IR spectra from silicate minerals with known anion structures provides some constraints on the structure of this polymerised interfacial silicate. Silicate minerals that have dimeric silicate anions ($Si_2O_7^{6-}$) have only one n(Si-O) band at > 1000 cm^{-1} which is due to the bridging Si-O-Si band. In more condensed silicates, the proportion of bridging Si-O-Si bonds increases at the expense of non-bridging Si-O bonds, the number of Si-O-Si stretching modes at >1000 cm^{-1} increases, and the maximum absorbance shifts to higher wavenumber. Cyclic silicates have been proposed as possible oligomeric species on iron oxide surfaces but they have strongly absorbing IR ring deformation modes between ~740 and 600 cm^{-1} that were not observed in this work. Silicates with polymerisation occurring in three dimensions have n(Si-O) modes at ~1100 cm^{-1} such as quartz and the amorphous $SiO_{2(am)}$ phase with their strongest bands at 1090 and 1110 cm^{-1}, respectively. The formation of a specific silicate oligomer on the ferrihydrite could be rationalised if the arrangement of adsorption sites on the ferrihydrite caused adjacent sorbed H_4SiO_4 monomers to be held in an orientation that is conducive to the formation of a condensed silicate species. All data are consistent with a model whereby a linear trimeric silicate species is formed on the iron oxide surface by the insertion of a H_4SiO_4 molecule from the solution phase between two suitably orientated adjacent sorbed monomers as illustrated in Fig. 2.

Solid state ^{29}Si NMR spectra

Solid state ^{29}Si NMR is a useful tool in the study of the structure of silicates because Si with different Q^n have distinct chemical shifts. Typical ^{29}Si shifts are -70 ± 4 ppm for isolated SiO_4 tetrahedra (Q^0), -80 ± 3 ppm for Q^1 such as dimers or the ends of linear chains, -87 ± 1 ppm for Q^2 such as in single silicate chains, -98 ± 1 ppm for Q^3 such as in silicate sheets and lastly -109 ± 2 ppm for Q^4.[28] However, the iron oxides are not amenable to NMR studies so an X-ray amorphous TiO_2 phase was produced by the hydrolysis of $Ti(OEt)_4$.[29] The TiO_2 and ferrihydrite phases are both composed of particles of approximately 2 nm diameter with very little long range order. The ATRIR spectra of H_4SiO_4 reacting on the TiO_2 surface showed the same progression from monomeric sorbed H_4SiO_4 to a polymerised species with the same spectral features as observed on the ferrihydrite.

A sample of TiO_2 was prepared with high G_{Si} using H_4SiO_4 solution prepared from ^{29}Si. The main peak in the NMR spectrum of this sample (Fig. 3) occurs at -87 ppm and there are clearly shoulders on either side of this peak, at -79.8 and -95.7 ppm. There is a low intensity tail extending on the more negative side of the peak at -105 ppm. The ^{29}Si NMR peak position for a Q^n Si depends primarily on the value of n but for Si with the same Q^n the peak position becomes more negative as the charge densities of the cations to which the silicates are associated increases.[30,31] Therefore to assign the peaks in the spectrum it is necessary to refer to materials where silicates are coordinated with Ti^{4+} cations. The peak at -79.8 ppm is within the range observed for Q^0 Si including the orthosilicate mineral titanite $CaTiSiO_5$ (-79.6 ppm). Similarly the peak at -95.7 ppm is within the range for Q^2 Si in sol–gel prepared mixed TiO_2–SiO_2 oxides (-92 to -96 ppm)[32,33] and in the cyclosilicate mineral benitoite (-94.2).[30] Only one reference value for Q^1 Si was found which was for a mixed TiO_2–SiO_2 oxide (-84 ppm)[32] and it is clear that the peak at -87 ppm is Q^1. The tail at -105 ppm indicates a small amount of silicate with Q^3–Q^4 but the peak is too weak to allow for definitive peak fitting. The NMR spectrum qualitatively agrees with the proposed model for H_4SiO_4 polymerisation at an oxide surface. The Q^0 peak corresponds to the monomeric adsorbed H_4SiO_4, while the Q^1 and Q^2 peaks correspond to terminal and middle Si in a linear silicate oligomer. The ratio of Q^1 and Q^2 peak areas would be 1:0.5 for a linear trimer which is in reasonable agreement with the measured value of 1:0.4.

Structural interpretation

The only condensed silicate species that is consistent with the ATRIR and ^{29}Si NMR spectra is a linear trimeric species. Furthermore the very similar ATRIR spectra for H_4SiO_4 condensation of ferrihydrite and amorphous TiO_2 suggests that the same silicate oligomerisation product is formed on the surface of two different poorly ordered oxides. This implies that this is a general phenomenon whereby bidentate silicate monomers on an oxide surface are disposed towards forming linear trimers by condensation reactions involving two terminal Si–OH groups.

In this section we demonstrate that this mechanism is structurally reasonable based on geometric constraints of silicate polymerisation and the structural model for amorphous TiO_2 that was developed by Zhang *et al.*[29] and for which the atomic coordinates were kindly provided.

In this structural model the TiO_2 particles contain 123 Ti atoms, 246 O atoms and have an irregular ''potato'' shape. The particles have a diameter of 2 nm with a small strained ''anatase-like'' core and a highly distorted shell. The average Ti coordination number was 5.3 due to the truncation of the many TiO_6 octahedra on the particle surface. In an aqueous suspension the surface will have a large number of terminal Ti–OH groups and there were 67 Ti ions on the particle surface that had a coordination number less than six and these Ti ions were considered to be surface active. The geometric constraints for surface silicate species were based on the range of Si–O bond distances and angles observed in silicate minerals. Liebau[34] gives Si–O distances between 1.57 and 1.72 Å, O–Si–O angles between 98 and 122° and Si–O–Si angles between 120 and 180°. The average distance between nearest neighbour surface Ti atoms is 3.1 ± 0.2 Å and 64 of the 67 surface active Ti ions have an adjacent site sufficiently close to be bridged by a H_4SiO_4 tetrahedra. To form a linear trimeric silicate requires adjacent monomers with an appropriate distance and orientation for insertion of a molecule of H_4SiO_4 in solution. Based on geometric constraints 54 of the surface Ti ions could be part of a site for linear trimer formation. This model of the surface is depicted in Fig. 4 which shows trimers can form on most of the particle surface. From this argument it would appear to be reasonable that oligomers can dominate the surface at high G_{Si}.

Finally, we discuss the observation that the TiO_2 surface is not predisposed to the formation of three dimensional polymers. Fig. 4 shows the relationship between adjacent adsorbed trimers. It is clear that adjacent trimers are orientated away from each other because of the high curvature of the surface of the small diameter TiO_2 particle. The distance between terminal hydroxide groups on the adjacent trimers range from 8 to 12 Å. This is too large to be bridged by a H_4SiO_4 molecule in solution and this prevents the formation of higher order silicate polymers. The similarity in the H_4SiO_4 oligomerisation chemistry on the poorly ordered oxides of both Ti^{IV} and Fe^{III} suggests the proposed interpretation of silicate oligomerisation may be more generally applicable to disordered surfaces, such as ferrihydrite. From simple geometric arguments nanometer sized oxide particles will have both a high curvature and also a high surface concentration of coordinatively unsaturated cations that will produce surface hydroxyl groups in water. These are the basic features of the proposed silicate oligomerisation model. While various structural models for ferrihydrite have been proposed and refuted, the $TiO_{2(am)}$ model indicates that nanometer sized particles with crystalline cores will tend to have a highly strained and disordered surface because of the constraints of high surface curvature. The primary particle size of ferrihydrite is 2–3 nm which is comparable to that of $TiO_{2(am)}$. In addition, the proposed concentration of monomer adsorption sites are comparable on the two oxides i.e. 0.26 per Ti for $TiO_{2(am)}$ and 0.2 per Fe for ferrihydrite. These structural and morphological similarities may explain the similar silicate surface chemistry on the ferrihydrite and $TiO_{2(am)}$.

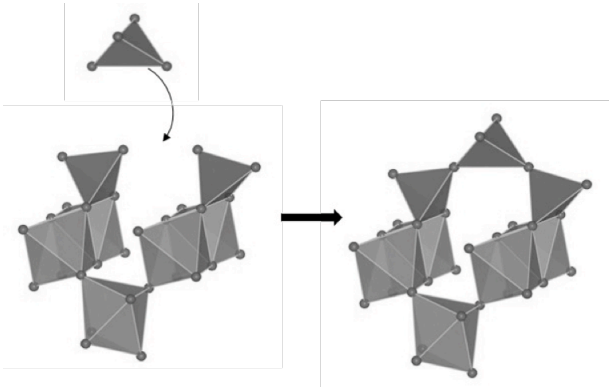

Fig 2. Model for the formation of surface oligomeric silicate species on an iron oxide surface. Tetrahedra are SiO_4 and octahedra are FeO_6.

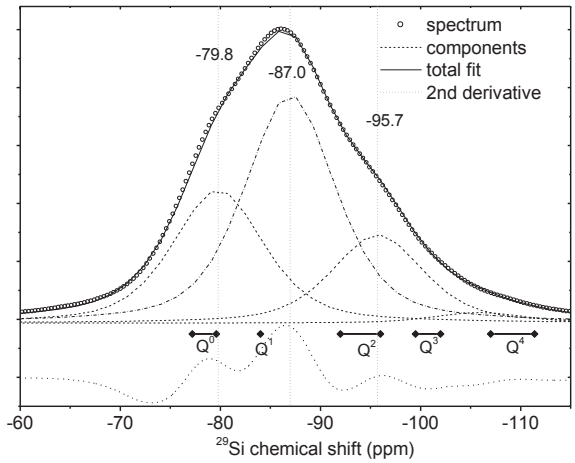

Fig 3. The ^{29}Si solid state NMR spectrum of $H_4{}^{29}SiO_4$ on TiO_2 at high G_{Si}. Reference values are for mineralogical samples and TiO_2-SiO_2 mixed phases.

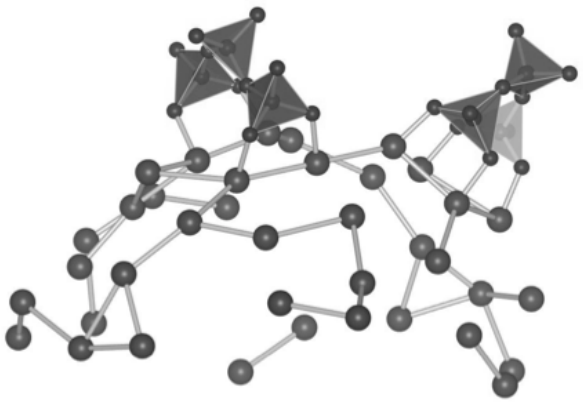

Fig. 4. The arrangement of Ti ions with coordination number < 6 on the surface of a $TiO_{2(am)}$ particle. Just the top half of the particle is shown. Lines between spheres depict sites where adjacent Ti ions are sufficiently close to allow bidentate coordination to SiO_4 tetrahedra. The tetrahedra in the figure depict two adjacent interfacial silicate trimers.

References

1. Goldschmidt, V. M. *Nature* **1929,** *124*, 15-17.
2. Rudnick, R. L.; Fountain, D. M. *Rev. Geophys.* **1995,** *33*, 267-309.
3. Filippou, A. C.; Baars, B.; Chernov, O.; Lebedev, Y. N.; Schnakenburg, G. *Angew. Chem. Int. Ed.* **2014,** *53*, 565-570.
4. Pauling, L. *Am. Miner.* **1980,** *65*, 321-323.
5. Weinhold, F.; West, R. *Organometallics* **2011,** *30*, 5815-5824.
6. Gustafsson, J. P. *Geoderma* **2006**, *136,* 320-330.
7. Aggett, J.; Roberts, L. S. *Env. Sci. Tech.* **1986,** *20*, 183-186.
8. Smith, A. H.; Lingas, E. O.; Rahmen, M. *Bull. WHO* **2000,** *78*, 1093-1103.
9. Carlson, L.; Schwertmann, U. *Geochim. Cosmochim. Acta* **1981,** *45*, 421-425.
10. Schwertmann, U.; Fechter, H. *Clay Min.* **1982,** *17*, 471-476.
11. Cornell, R. M.; Giovanoli, R. *J. Chem. Soc. Chem. Comm.* **1987**, *6,* 413-414.
12. Cornell, R. M.; Giovanoli, R.; Schindler, P. W. *Clays Clay Min.* **1987,** *35*, 21-28.
13. Kwon, S.-K.; Shinoda, K.; Suzuki, S.; Waseda, Y. *Corrosion Sci.* **2007,** *49*, 1513-1526.
14. Davis, C. C.; Knocke, W. R.; Edwards, M. *Env. Sci. Tech.* **2001,** *35*, 3158-3162.
15. Corrias, A.; Ennas, G.; Mountjoy, G.; Paschina, G. *Phys. Chem. Chem. Phys.* **2000,** *2*, 1045-1050.
16. Kwon, S. K.; Kimijima, K.; Kanie, K.; Suzuki, S.; Muramatsu, A.; Saito, M.; Shinoda, K.; Waseda, Y. *Corrosion Sci.* **2007,** *49*, 2946-2961.
17. Davis, C. C.; Chen, H.-W.; Edwards, M. *Env. Sci. Tech.* **2002,** *36*, 582-587.
18. Swedlund, P. J.; Sivaloganathan, S.; Miskelly, G. M.; Waterhouse, G. I. N. *Chem. Geol.* **2011,** *285*, 62-69.
19. Knight, C. T. G.; Balec, R. J.; Kinrade, S. D. *Angew. Chem. Int.* **2007,** *46*, 8148 –8152.
20. Alvarez, R.; Sparks, D. L. *Nature* **1985,** *318*, 649-651.
21. Svensson, I. L.; Sjoberg, S.; Ohman, L. O. *J. Chem. Soc. Faraday Trans.* **1986,** *82*, 3635-3646.
22. Felmy, A. R.; Cho, H.; Rustad, J. R.; Mason, M. J. *J. Solution Chem.* **2001,** *30*, 509-525.
23. Peak, D.; Ford, R. G.; Sparks, D. L. *J. Colloid Interface Sci.* **1999,** *218*, 289-299.
24. Farmer, V. C. In *Infrared Spectra of Minerals;* Farmer, V. C. Ed.; Mineralogical Society , London, Monograph No. 4, 1974.
25. Lazarev, A. N. *Vibrational spectra and structure of silicates*; Consultants Bureau: New York, 1972.
26. McIntosh, G. J.; Swedlund, P. J.; Sohnel, T. *Phys. Chem. Chem. Phys.* **2011,** *13*, 2314-2322.
27. Pokrovski, G. S.; Schott, J.; Garges, F.; Hazemann, J. L. *Geochim. Cosmochim. Acta* **2003,** *67*, 3559-3573.
28. Lippmaa, E.; Maegi, M.; Samoson, A.; Engelhardt, G.; Grimmer, A. R. *J. Am. Chem. Soc.* **1980,** *102*, 4889-4893.
29. Zhang, H. Z.; Chen, B.; Banfield, J. F.; Waychunas, G. A. *Phys. Rev. B* **2008,** *78*, 214106.
30. Stebbins, J. F. In *Mineral physics & crystallography : a handbook of physical constants;* Ahrens, T. J. Ed.; American Geophysical Union: Washington DC, 1995.
31. Stebbins, J. F. *MRS Bulletin* **1992,** *17*, 45-52.
32. Dirken, P. J.; Smith, M. E.; Whitfield, H. J. *J. Phys. Chem.* **1995,** *99*, 395-401.
33. Tada, H.; Akazawa, M.; Kubo, Y.; Ito, S. *J. Phys. Chem. B* **1998,** *102*, 6360-6366.
34. Liebau, F. *Structural chemistry of silicates : structure, bonding, and classification*; Springer-Verlag: Berlin, 1985.